Rendering of inhomogeneous volumes using perturbation functions

Olexandr Romanyuk[*a], Oksana Romanyuk[a], Roman Chekhmestruk[b], Pavlo Mykhaylov[c], Mariana Kovtonyuk[d], Iryna Baranovska[d], Svitlana Nahorniak[e], Olena Hrechanovska[a], Zbigniew Omiotek[f], Aida Uvaysova[f]

[a]Vinnytsia National Technical University, Vinnytsia, Ukraine; [b]3D GENERATION UA, 37, Vinnytsia, Ukraine; [c]CEO 3D GNERATION GmbH, Dortmund, Germany; [d]Vinnytsia Mykhailo Kotsiubynskyi State Pedagogical University, Vinnytsia, Ukraine; [e]Vinnytsia Cooperative Institute, Vinnytsia, Ukraine; [f]Lublin University of Technology, Lublin, Poland

ABSTRACT

A method for rendering inhomogeneous volumes using perturbation functions is presented. An approach is proposed for sampling light transmission paths in heterogeneous media. At the initial stage of calculations, light transmission paths are constructed in a closed form. Then the heterogeneous component is averaged by adding a formal medium. Next, the path-tracking algorithm is used. Due to this, there is no need to calculate strict boundaries of the attenuation function. Samples in the closed-form light transmission path and the averaged medium are made separately. This minimizes the costly calculations of collision coefficients that change when traversing space.

Keywords: perturbation functions, inhomogeneous volume, rendering, sampling, transmission coefficient, path tracking

1. INTRODUCTION

Modelling of light transmission in heterogeneous volumes is of great importance in many fields, such as medical imaging, scientific visualization and synthesis of realistic images. Visual effects uses complex three-dimensional structures such as smoke and clouds. However, modelling light transmission requires many calculations. For example, Monte Carlo methods, which are based on path tracing, require the construction of a huge number of light paths. At the same time, each light path consists of thousands of scattering parts. The propagation of light in the medium is described by the radiation transfer equation[1,2]. The radiation transfer equation relates the change in the radiation energy to the collision coefficients of the medium. Which include the absorption coefficient, the scattering coefficient, their sum, and the extinction coefficient. Stochastic particle trajectories have been developed for the numerical solution of the radiation transfer equation. These are the direct flight paths of particles between subsequent collisions with the medium. These paths can be selected using reverse transformation sampling[3-5]. If the cumulative distribution function is analytically invertible, then the free span distance can be chosen analytically. It is possible to find a solution iteratively, using Newton's method. The Monte Carlo method was also developed for direct sampling of flight paths in environments with continuously varying cross-sections[6-9]. This method is an alternative to the delta tracking approach. It is used for tasks in which the cross-sections of the material vary depending on the flight paths of the particles. The method has advantages for calculations of charged particles by the Monte Carlo method, atmospheric transport, radiation transfer, transport through stochastic media, and so on. In works [10-12], the physical principles and approximations used in Monte Carlo simulation are considered. Theoretical models and approximations leading to differential cross sections used in Monte Carlo codes are described. Monte Carlo simulation is becoming more and more complex. The most widely used tracking method, ray tracing has serious drawbacks. Delta tracking is the most common alternative[13-16].

However, the method is not stable enough, since its effectiveness strongly depends on the models. A hybrid tracking method is presented in works [17-19]. Hybrid tracking increases computational efficiency by combining cells into complex geometric models. The articles [20, 21] describe a grid-based ray casting method for visualizing isosurfaces of binary volumes. A multi-level data structure is used. This data structure is used to improve the performance of the ray-casting algorithm. A grid-based Monte Carlo algorithm is also presented to support various methods of wide-field illumination.

*rom8591@gmail.com

Photonics Applications in Astronomy, Communications, Industry, and High Energy Physics Experiments 2022, edited by Ryszard S. Romaniuk, Andrzej Smolarz, Waldemar Wójcik, Proc. of SPIE Vol. 12476, 124760O

The algorithm can also simulate wide field detectors. The flexibility of source and detector modelling is achieved through a fast grid recalculation process. The calculation combines the target area and the source / detector space in a single tetrahedral grid. A modified Monte Carlo algorithm is also proposed that simultaneously evaluates the physical observable A and the derivatives of A for each parameter of the problem. The Monte Carlo method treats A as the expectation of a random variable. Expectation is an integral. The integral is output as a function of the problem parameter to obtain a new integral. The new integral, in turn, can be estimated using the Monte Carlo method. Zero collision algorithms work well with radiation transmission in heterogeneous media. However, they give rise to convergence difficulties when considering sensitivity estimates. In work [10], rendering without assumptions is described using the ray marching method to estimate the transmission coefficient. These are optical modelling for realistic image synthesis taking into account 3D scenes, optimisation on a physical basis for the design and manufacture of artificial objects taking into account desirable functions regulated by physical laws, hydrodynamics, and so on. In delta tracking methods, a fictitious environment is introduced, represented by a zero collision coefficient, with the help of which the total collision density is averaged. This is necessary to ensure analytical sampling of free trajectories in a heterogeneous environment. The main disadvantage of delta tracking is a large number of expensive searches for volume parameters changing in space.

2. DESCRIPTION OF THE METHOD

2.1 Volume boundaries based on perturbation functions

The objects are defined using second-order surfaces - quadrics and 2nd-order perturbation functions: F'(x,y,z) = F(x,y,z) + R(x,y,z), where the perturbation function R(x,y,z) is as follows[13]:

$$R(x,y,z)=\begin{cases} Q^2(x,y,z), if\ \ Q(x,y,z)>0 \\ 0, if\ \ Q(x,y,z)\le 0, \end{cases}, \tag{1}$$

where Q(x,y,z) is a perturbing quadric.

A second-order three-dimensional function is defined by ten coefficients. The same amount of data is needed to describe the spatial location of one triangular face. A more compact representation of the model allows you to reduce memory costs when storing a database, and, consequently, to unload the transport routes between the computing components of the system and memory blocks. On the other hand, it becomes possible to design smooth objects without the defects inherent in polygonal models. A class of free forms is built on this basis. This means the ability to describe complex geometric objects by specifying a second-order deviation function from the base surface. In addition, during image generation, only the coefficients of the bearing surface must be subjected to geometric transformations, because the deviation function remains constant, thus reducing the load on the geometric processor.

The surface of a quadric is a surface of a constant level of a second-order function Q(x, y, z). Let's define a certain perturbation function, R(x, y, z), which has the smoothness property. Now consider the function F(x, y, z) = Q(x, y, z) + R(x, y, z). Due to the smoothness of R and Q, F will retain this property, and, consequently, the surface of level zero will be smooth. Thus, we have constructed a complex surface using a second-order function as the base one. However, to get the desired shape of the surface, you need to learn how to set the appropriate perturbation function in an acceptable way. A smooth perturbation is constructed from a quadratic function as follows. Let's define the inner region of Q as a part of the space where 0 < Q. Then the outer part of the Q put R equal to zero, and in the inner part will construct Q in a square (1).

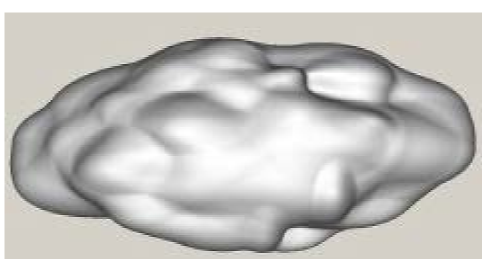

Figure 1. The volume bounded by the disturbed surface.

In addition, the object that we call a free form, remains essentially a quadric, but considering the addition made by the disturbance to their own basic functions (Fig. 1). In turn, the free form may be a function of the perturbation for any other object. Radiation transfer equation in differential form[14]:

$$(\omega\cdot\nabla)L(\vec{x},\omega) = -\mu_t(\vec{x})L(\vec{x},\omega) + \mu_a(\vec{x})L_e(\vec{x},\omega) + \mu_s(\vec{x})\int_{S^2} f_p(\omega,\varpi)L(\vec{x},\varpi)d\varpi \ , \tag{2}$$

where $L(\vec{x},\omega)$ is a radiation parameterised by the point $\vec{x}$ and direction of motion ω, $\mu_t(\vec{x})L(\vec{x},\omega)$ is the losses caused by absorption and scattering, and $\mu_a(\vec{x})L_e(\vec{x},\omega)$ and $\mu_s(\vec{x})\int_{S^2} f_p(\omega,\varpi)L(\vec{x},\varpi)d\varpi$ are the gains caused by radiation $L_e(\vec{x},\omega)$ and scattering, $f_p(\omega,\varpi)$ is a phase function quantifies the directional density of scattered light.

By solving the Dirac integral, an integral form of the radiation transfer equation is obtained, including zero collisions:

$$L(\vec{x},\omega) = \int_0^\infty \exp\left(-\int_0^t \mu_t(\vec{x}_s) + \vec{\mu}_n(\vec{x}_s)ds\right)\times\left[\ \mu_a(\vec{x}_t)L_e(\vec{x}_t,\omega) + \mu_s(\vec{x}_t)L(\vec{x}_t,\omega)\ \right]dt\ , \tag{3}$$

where $\vec{x}_t = \vec{x} - t\omega$ and $\vec{x}_s = \vec{x} - s\omega$.

For tracking algorithms in heterogeneous environments, identities are introduced that translate equation (3) directly into the code for its solution. By replacing integrals with Monte Carlo estimates, the radiation transfer equation is directly translated into a set of recursive algorithms. Figure 2 shows a light path in a heterogeneous medium, along which absorption, scattering and zero collisions occur.

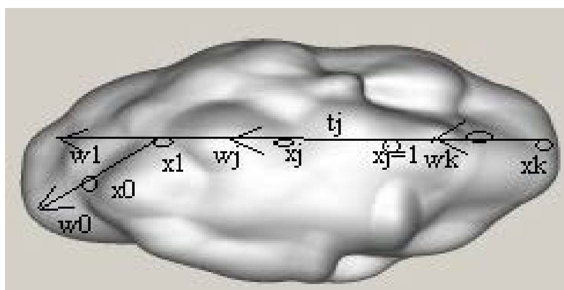

Figure 2. The light path in a heterogeneous medium.

It is possible to lower the variance and reduce access to memory due to analytical processing of a homogeneous part of the volume. To do this, the initial volume is decomposed into homogeneous and heterogeneous parts.

2.2 Path tracking

Equation (3) can be rewritten for a medium with k absorbing and scattering components:

$$L(\vec{x},\omega) = \int_0^\infty \exp\left(-\int_0^t \sum_{j=1}^{k}\ \mu_t^j(\vec{x}_s) + \vec{\mu}_n(\vec{x}_s)ds\right)\times\left[\sum_{j=1}^{k}\mu_a^j(\vec{x}_t)L_e(\vec{x}_t,\omega) + \sum_{j=1}^{k}\mu_s^j(\vec{x}_t)L_s(\vec{x}_t,\omega) + \mu_n(\vec{x}_t)L(\vec{x}_t,\omega)\right]dt\ , \tag{4}$$

where j is an index of the individual components.

After including probabilities and probabilistic estimation, there will be:

$$\begin{aligned} L(\vec{x}_i,\omega_i) = \int_0^\infty p(t_i)\times\Bigg[&\sum_{i=1}^{k}\int_0^1 H\left[\varsigma_e^j < P_a^j(\vec{x}_+)\right]\times\frac{\mu_a^j(\vec{x}_+)}{\bar{\mu}_+ P_a^j(\vec{x}_+)}L_e(\vec{x}_+,\omega_i)d\varsigma_e^j + \\ &+\sum_{i=1}^{k}\int_0^1\ H\left[\varsigma_s^j < P_s^j(\vec{x}_+)\right]\frac{\mu_s^j(\vec{x}_+)}{\bar{\mu}_+ P_s^j(\vec{x}_+)}L_s(\vec{x}_t,\omega_i)d\varsigma_s^j + \int_0^1\ H\left[\varsigma_n < P_n(\vec{x}_+)\right]\frac{\mu_n(\vec{x}_+)}{\bar{\mu}_+ P_n(\vec{x}_+)}L(\vec{x},\omega_i)d\varsigma_n\Bigg]dt_i \end{aligned}, \tag{5}$$

where $P_a(\vec{x})$, $P_s(\vec{x})$, $P_n(\vec{x})$ are probabilities. H is the Heaviside function.

Probability density function:

$$p(t) = \bar{\mu}(\vec{x}_t)\exp\left(-\int_0^t \bar{\mu}(\vec{x}_s)ds\right). \tag{6}$$

$\bar{\mu}(\vec{x}) = \mu_t(\vec{x}) + \mu_n(\vec{x})$ is a sampling coefficient of the free path, it combines the coefficients of attenuation and zero collision; $\mu_a(\vec{x}) \in [0,\infty)$ is an absorption coefficient of the initial volume; $\mu_s(\vec{x}) \in [0,\infty)$ is a scattering coefficient of the initial volume; $\mu_t(\vec{x}) = \mu_a(\vec{x}) + \mu_s(\vec{x})$ is an attenuation coefficient of the initial volume; $\mu_a^u \in [0,\infty)$ is an absorption coefficient of the homogeneous part of the volume; $\mu_s^u \in [0,\infty)$ is a scattering coefficient of the homogeneous part of the volume; $\mu_t^u = \mu_a^u + \mu_s^u$ is an attenuation coefficient of the homogeneous part of the volume; $\mu_a^h(\vec{x}) = \mu_a(\vec{x}) - \mu_a^u(\vec{x})$ is an absorption coefficient of the inhomogeneous part of the volume; $\mu_s^h(\vec{x}) = \mu_s(\vec{x}) - \mu_s^u(\vec{x})$ is a scattering coefficient of the inhomogeneous part of the volume; $\mu_t^h(\vec{x}) = \mu_t(\vec{x}) - \mu_t^u(\vec{x})$ is an attenuation coefficient of the inhomogeneous part of the volume; $\bar{\mu} \in (\mu_t^u, \infty)$ is a path sampling coefficient; $\mu_n(\vec{x}) = \mu - \mu_t^u - \mu_t^h(\vec{x})$ is zero collision coefficient.

Probabilities of sampling a homogeneous part, with constant coefficients:

$$P_a^u = \frac{\mu_a^u}{\bar{\mu}}, \tag{7}$$

$$P_s^u = \frac{\mu_s^u}{\bar{\mu}}. \tag{8}$$

3. RESULTS

The results of the work are integrated into the path tracer. We use objects based on perturbation functions as an acceleration structure. The empty space is determined and approximate local extremes of the base volumes are stored. Objects based on perturbation functions adapt to volume uniformity. Voluminous data sets based on voxels are stored.

Performance is compared using the number of queries, visualization time, root mean square error and metrics, that is, the search in units of variance. The variance is calculated as the product of the number of searches and the variance. For all of the above indicators, lower values mean better performance. Calculations were performed on Intel Xeon E5-2678 v3 (the number of cores is 12, the number of threads is 24, the base frequency is 2.5 GHz).

Figure 3 shows a cloud with a functionally defined three-dimensional object inside with a phase function $\alpha = 1$, and with an octal tree depth of eight. The number of searches is most reduced in the inner part of the cloud, where the fading changes less. Table 1 shows the effect of the depth of the octal tree on performance, as the depth increases, the calculation time increases. Table 1 also shows a decrease in the calculation time of path tracking as the depth increases.

Increasing the depth allows path tracking to reduce the search more efficiently, as the volume inside each leaf of the octal tree becomes uniform. A depth of eight to ten provides a good balance. Tracking the path reduces the overall rendering time, since traversing the octal tree, sampling, and other overhead costs take considerable time.

Table 1. The effect of the depth of the octal tree on performance.

Depth of the octal tree	4	8	16
Increase in the calculation time of the octal tree (by the number of times)	4.92	11.47	14.31
Reducing the calculation time of path tracking (by the number of times)	4.34	20.42	19.02

Figure 3 shows a diagram of the increase in the calculation time of an octal tree. Figure 4 shows a diagram of the decrease in the calculation time of path tracking.

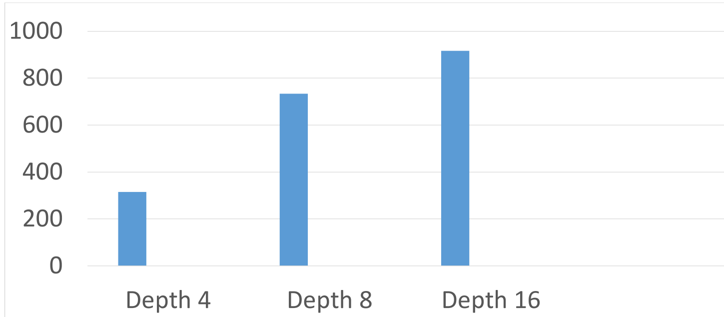

Figure 3. Increasing the calculation time of the octal tree.

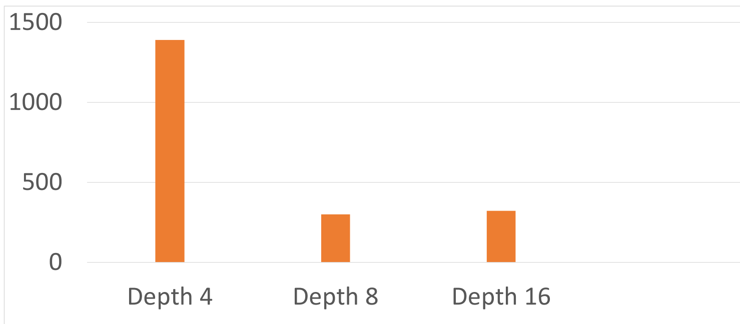

Figure 4. Reducing the calculation time of path tracking.

4. CONCLUSIONS

A method for rendering inhomogeneous volumes using perturbation functions is presented. To reduce costs, modelling of light transfer in inhomogeneous volumes is proposed. The methods provide high performance and efficiently handle collision coefficients. The approach is derived from the radiation transfer equation, using the integral formulation of the zero collision algorithm. The effectiveness of path tracking depends on how tightly the extinction coefficient can be limited. This is a difficult task for a high degree of volume heterogeneity. Performance depends on how well the spatial structure isolates and subdivides heterogeneous regions. We apply bounding shells based on perturbation functions. An important feature of the method is the ability to process unlimited sampling coefficients of free run and control attenuation. Path tracking is well suited for situations where memory retrieval is expensive. In addition, if the datasets are large and subject to cache overload. Alternatively, expensive high-order interpolation is used. Additionally, if the volume is modelled with complex procedural functions, the savings can be significant. The method is also effective for arbitrary values of collision coefficients if the sampling coefficient of the free run limits the extinction coefficient. In our opinion, the method is relevant for computer graphics. Its application will stimulate further research in visualization applications.

REFERENCES

[1] Mayer, B., "Radiative transfer in the cloudy atmosphere," The European Physical Journal Conferences 1, 75-99 (2009).

[2] Reiter, D., "The Monte Carlo Method, an Introduction," Lecture Notes in Physics 739, 63-78 (2007).

[3] Ueki, T., "Monte Carlo criticality analysis under material distribution uncertainty," Project: Criticality Analysis under Material Distribution Uncertainty, Journal of Nuclear Science and Technology 54(3), 267-279 (2017).

[4] Salvat, F., Fernandez-Varea, J. M., "Overview of physical interaction models for photon and electron transport used in Monte Carlo codes," Metrologia 46(2), 112 (2009).

[5] Liu, M., Guo, Y. Ma, X., Liu, S., "An improved tracking method for particle transport Monte Carlo simulations," Journal of Computational Physics 437(5), (2021).

[6] Li, W., Hahn, J. K., "Efficient ray casting polygonized isosurface of binary volumes," The Visual Computer, Springer, (2021).
[7] Yao,R., Intes,X., Fang, Q., "Generalized mesh-based Monte Carlo for wide- field illumination and detection via mesh retessellation," Projects: Compressive Optical Tomography with Structured LightMesh-based Monte Carlo, Biomedical Optics Express 7(1), 171-184 (2015).
[8] Barnat-Hunek, D., Omiotek, Z., Szafraniec, M., Dzierżak, R., "An integrated texture analysis and machine learning approach for durability assessment of lightweight cement composites with hydrophobic coatings modified by nanocellulose," Measurement 179, 1-20 (2021).
[9] Tregan, J.-M., Blanco, S., Dauchet, J., Mouna, E. H., "Convergence issues in derivatives of Monte Carlo null-collision integral formulations: A solution," Journal of Computational Physics 413(11), (2020).
[10] Kettunen, M., d'Eon, E., Pantaleoni, J., Novak, J., "An unbiased ray-marching transmittance estimator," ACM Transactions on Graphics 40(4), 1-20 (2021).
[11] Yue, Y., "Bringing Computer and Physics Closer," Journal of Physics Conference Series 1036(1), (2018).
[12] Olexandr, R. Vyatkin, N., Mykhaylov, S. I., Chekhmestruk, P. I., "Interactive shape modeling using functionally defined objects," Herald of Advanced Information Technology 3(3), 149-163 (2020).
[13] Fasso, A., Ferrari, A., Sala, P., "Radiation transport calculations and simulations," Radiation Protection Dosimetry 137(1-2), 118-33 (2009).
[14] Rovira, R. H., Pavlov, S. V., Kaminski, O.S., Bayas, M. M., "Methods of Processing Video Polarimetry Information Based on Least-Squares and Fourier Analysis," RH - Middle-East Journal of Scientific Research 16(9), 1201-1204 (2013).
[15] Zabolotna, N. I., Pavlov, S. V., Ushenko, A. G., Sobko, O. V., Savich, V. O., "Multivariate system of polarization tomography of biological crystals birefringence networks," Proc. SPIE 9166, (2014).
[16] Omiotek, Z., Kotyra, A., "Flame image processing and classification using a pre-trained VGG16 model in combustion diagnosis," Sensors 21(2), 1-15 (2021).
[17] Wajman, R., and Banasiak, R., "New tunnel based method of sensitivity matrix calculation for 3D capacitance tomography image reconstruction," Informatyka, Automatyka, Pomiary w Gospodarce i Ochronie Środowiska 3(3), 32-37 (2013).
[18] Kvyetnyy, R. N., Romanyuk, O. N., Titarchuk, E. O., et al., "Usage of the hybrid encryption in a cloud instant messages exchange system," Proc. SPIE 10031 (2016).
[19] Vyatkin, S. I., Romanyuk, S. A., Pavlov, S. V., Wójcik, W., et al., "Using lights in a volume-oriented rendering," Proc. SPIE 10445, (2017).
[20] Romanyuk, O. N., Pavlov, S. V., Melnyk, O. V., Romanyuk, S. O., Smolarz, A., et al., "Method of anti-aliasing with the use of the new pixel model," Proc. SPIE 9816, (2015).
[21] Romanyuk, S. O., Pavlov, S. V., Melnyk, O. V., "New method to control color intensity for antialiasing," Control and Communications (SIBCON), 2015 International Siberian Conference, (2015).